

## Binding Pattern Analysis of Different Allosteric Inhibitors of Hepatitis C Virus (HCV) Polymerase

Marium Bibi\*

Department of Biosciences, Shaheed Zulfikar Ali Bhutto Institute of Science and Technology Block 5, Clifton, Karachi-75600, Pakistan.

[dr.marium@szabist.edu.pk](mailto:dr.marium@szabist.edu.pk)\*

(Received on 17<sup>th</sup> April 2023, accepted in revised form 16<sup>th</sup> June 2023)

**Summary:** To the best of our knowledge, the current study could be considered the first comprehensive one based on the application of molecular docking on the non-nucleoside thumb and palm inhibitors to nonstructural NS5B protein for the detailed evaluation of their binding patterns in the corresponding binding regions in the protein. Non-nucleoside thumb and palm inhibitors were docked into the thumb and palm sites of the nonstructural NS5B protein which is the RNA-dependent RNA polymerase, respectively. Two docking programs, AutoDock 4.2 and AutoDock Vina were employed for the docking of thumb inhibitors (filibuvir and lomibuvir) and palm inhibitors (dasabuvir and nesbuvir) into the respective binding region. The preliminary analysis of the docking performance demonstrated that AutoDock Vina was suitable for the docking of large flexible molecules as deduced from the alignment of docking conformations in all cases. Based on the docking calculation, the interaction pattern analysis was carried out for all the inhibitors which were found to reside in the respective binding region. Before the interaction pattern analysis, the best docking pose was selected based on the high binding affinity value. The interaction pattern analysis of the inhibitors revealed that hydrogen bonding and hydrophobic contacts with amino acid residues of the respective binding region were the leading force in the stabilization of these inhibitors besides other interactions. The interaction pattern analysis based on the docking calculation was also realized to be the meaningful approach to figuring out the relative stability of the protein-ligand complex formed after the inhibitor binding which eventually led to assessing the inhibitory potential of these inhibitors and could also be helpful for the future inhibitor design.

**Keywords:** Non-nucleoside inhibitors, NS5B protein, Molecular docking, Hydrogen bonding, Hydrophobic contacts.

### Introduction

Hepatitis C is a liver infection caused by the hepatitis C virus (HCV) which poses serious threats to global health leading to liver cancer that is characterized as cirrhosis and hepatocellular carcinoma (HCC)[1]. HCV infection persists for a short duration, however, more than half of people are exposed to a long-term chronic infection that ends up in cirrhosis and liver cancer. People with chronic infection can also have no symptoms appearing as healthy, which causes them to be unaware of or to ignore the disease which results in a devastating situation with advanced liver disease. It is also pertinent to mention here that no vaccine is available for HCV infection and only precaution can help escape from the disease in particular by injecting drugs. Fast diagnostics for HCV infection also help for the cure, since treatments can be effective only for the infection stage within 8 to 12 weeks.

HCV is a small, enveloped, and positive-sense single-stranded RNA virus that belongs to the

family *Flaviviridae*. The HCV particle has an envelope composed of a lipid membrane that embeds two glycoproteins, E1 and E2, which help the virus to attach and thus enter the cell[2-4]. The envelope is structurally an icosahedral core that contains RNA material. The RNA of HCV has the 5' and 3' ends along with the untranslated region, which plays a significant role in the translation and replication of the viral RNA. The 5' untranslated region has a ribosome binding site or internal ribosome entry site (IRES) that initiates the translation of a large protein that is later cleaved by cellular and viral proteases into the 10 different small proteins thus allowing viral replication within the host cell, and to assemble into the mature viral particles[5]. The structural proteins made by the HCV virus include core proteins, E1 and E2, whereas nonstructural proteins are NS2, NS3, NS4A, NS4B, NS5A, and NS5B[6]. Among these, the NS5B protein is the RNA-dependent RNA polymerase that has the key function of replication using the viral positive sense RNA strand as its template and catalyzes the

---

\*To whom all correspondence should be addressed.

polymerization of ribonucleoside triphosphates (rNTP)[7-9]. The therapeutic potential of NS5B polymerase is established due to its potential utilization of an RNA template that is not present in mammalian host cells[10]. The NS5B polymerase has adopted a right-hand topology in a three-dimensional conformation comprising finger, palm, and thumb domains, and the active site is located in the palm domain[11, 12]. The discovery of NS5B inhibitors is based on the binding of different ligands to these domains as reported by different crystal structures[13]. The NS5B inhibitors are reported to be non-nucleoside inhibitors (NNIs) and nucleoside inhibitors (NIs) that are established based on their mode of action as NIs compete for the RNA interaction with the nucleoside triphosphate mimicking the substrate of the enzyme which in turn interferes the RNA chain replication and elongation, whereas NNIs bring conformational changes after binding to the allosteric site of the thumb or palm domain thus deforming the shape of the active site optimally required for the enzymatic activity[14, 15].

The quest for antiviral compounds against HCV infection is being carried out with great endeavors due to its ever-spreading and high infection rate, therefore, experimental as well as computational methods have been applied to this cause for a long time. Numerous studies which have been reported on the synthesis of NS5B inhibitors with their biological activities are not possible to mention here. However, very few recent studies are mentioned here; for instance, the synthesis and biological activity of 2-(3,4-dimethyl-5,5-dioxidobenzo[e]pyrazolo[4,3-c][1,2]thiazin-2(4H)-yl)-N-(2-fluorobenzyl)acetamide, a new HCV NS5B polymerase inhibitor have been carried out, and computational studies based on molecular docking and a very short molecular dynamics simulation have also been applied to evaluate of the binding mode of the inhibitor. A combined study based on 3D-QSAR, molecular docking, and molecular dynamics study was reported on the benzimidazole derivatives which inhibit NS5B polymerase, and NNIs bearing a fused benzofuran scaffold were also tested against NS5B polymerase[16-18]. These are just a few examples that are reported in the literature on the discovery of new NS5B polymerase inhibitors which consist of NIs and NNIs. Our study focuses only on the binding analysis of different allosteric NS5B polymerase inhibitors (lomibuvir and filibuvir, and dasabuvir and dasabuvir) since these inhibitors have been reported to be effective against different genotypes of NS5B such as 1b (BK and Con1) and 3a as reported based on

biophysical techniques and a novel biosensor-based real-time polymerase assay to investigate their mode of action and selectivity of these inhibitors against enzyme from genotypes 1b (BK and Con1) and 3a[19]. For this purpose, an attempt was made by utilizing molecular docking of these inhibitors against NS5B polymerase genotype 1b which is expected to pave the way for developing an understanding of the binding mode of these inhibitors against other NS5B polymerase genotypes.

## Experimental

Before performing molecular docking, these compounds were optimized using the semi-empirical PM3 method which resulted in the optimized structures shown in Fig. 1 [20, 21]. These compounds were then subjected to docking calculations against the NS5B polymerase enzyme. The enzyme has been reported to have three distinct domains regarded as finger, palm, and thumb domains, with the active site located in the palm domain (Fig. 2). The compounds have already been reported to be thumb (lomibuvir and filibuvir) and palm (dasabuvir and nesbuvir) inhibitors, therefore, the crystal structures should be available for the NS5B polymerase with co-crystallized ligand bound to the thumb and palm regions of the enzyme, for instance, the structure of NS5B 1b (BK) complexed with filibuvir is deposited in the protein databank with PDB ID: 3FRZ which showed that filibuvir occupies the thumb region of the enzyme[22]. At first, the re-docking of filibuvir has been performed in the thumb region of the enzyme which was followed by the docking of lomibuvir to the same region of the enzyme.

A similar approach was adapted for the docking of palm inhibitors by retrieving a complex structure of a substituted benzothiadiazine bound to the palm domain of the enzyme from the protein databank (PDB: 3HHK)[23]. First of all, the co-crystallized substituted benzothiadiazine was subjected to re-docking calculation into the palm region of the enzyme that was then followed by the docking calculation of the reported palm inhibitors (dasabuvir and nesbuvir). For the molecular docking calculations, two docking programs AutoDock 4.2 and AutoDock Vina were employed using the following docking protocols[24, 25].

*AutoDock 4.2 docking protocol:* The docking of co-crystallized ligand "filibuvir" was carried out into the thumb region of the enzyme and for this purpose, the centroid of the ligand was obtained from

the complex (PDB ID: 3FRZ) which came out to be X 12.769, Y 34.617, Z 21.075 Å. Afterward, the ligand was extracted from the complex and subjected to the docking calculations using the above-mentioned programs with the help of AutoDockTools which is a GUI for performing the molecular docking which integrates both docking programs. For the docking, the rigid docking approach was implemented which consists of hydrogenation and the charge assignment that is Gastegier and Kollman charges to the inhibitors and the protein, respectively. The torsions of both ligands (filibuvir and lomibuvir) were adjusted using the default setting and the maximum limit of freedom for torsional degrees was set with a 2.0 root mean square deviation tolerance limit. Based on the centroid (PDB ID: 3FRZ), the grid mapping was performed by setting the grid parameters for the ligand binding based on the centroid coordinates for the grid points, with the box size of side lengths of 40 Å for each axis. The protein was set rigid for neglect to eliminate misleading interactions with the small ligands using Lamarckian Genetic Algorithms (LGA) for the binding energy calculations. Other parameters include

the local search space with a 300 iteration limit using 1.0 maximum size, the change in the step size from gene to the gene was controlled through pseudo-Solis and Wets parameters, and the maximum conformations limit was set to 30. Similarly, the docking of lomibuvir was carried out into the thumb domain of the enzyme using the same docking parameters.

For the docking of palm inhibitors, the co-crystallized substituted benzothiadizine bound to the palm region of the enzyme was extracted from the complex (PDB ID: 3HHK). The centroid information was obtained based on the crystal structure which yielded to be X 95.548, Y 45.591, Z 51.000 Å that was used for the docking of the co-crystallized benzothiadizine derivative, and dasabuvir and nesbuvir into the palm domain of the enzyme. The rest of the docking procedure and parameters were the same as those adapted for the docking calculations of the thumb inhibitors.

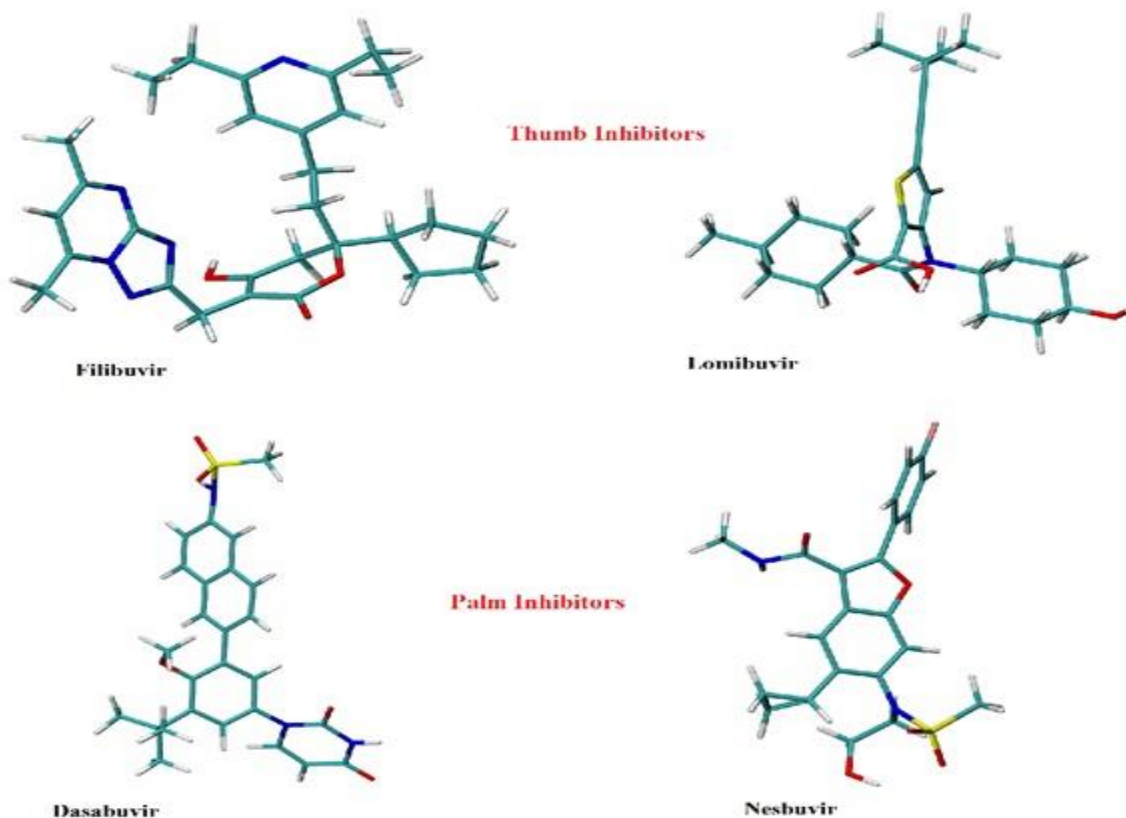


Fig. 1: 3D-structure of the inhibitors obtained from geometry optimization employing the semi-empirical PM3 method.

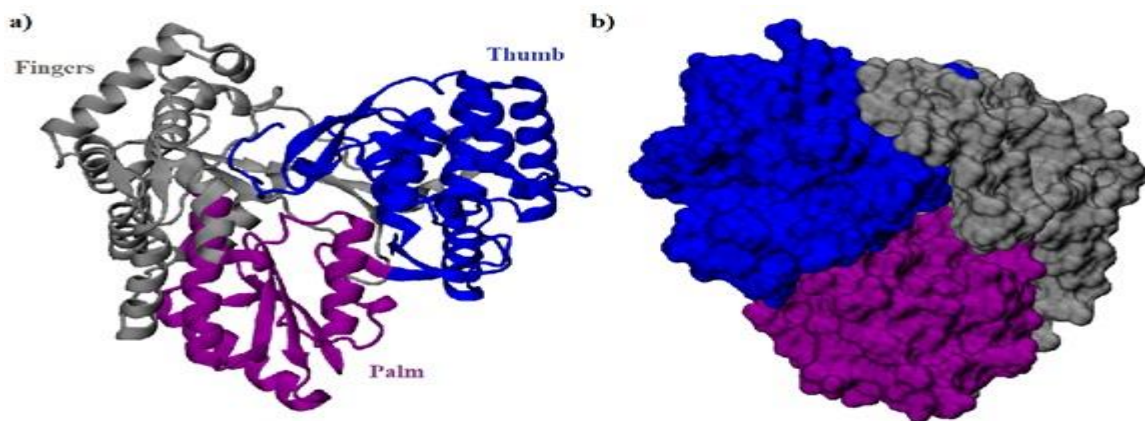


Fig. 2: Overall views of HCV NS5B polymerase in a) ribbon representation showing different domains colored according to thumb (blue; residues 371 to 563), palm (purple; residues 188 to 227 and 287 to 370), and fingers (grey; residues 1 to 187 and 228 to 286), and b) molecule surface of NSB5, rotated  $\sim 90^\circ$ .

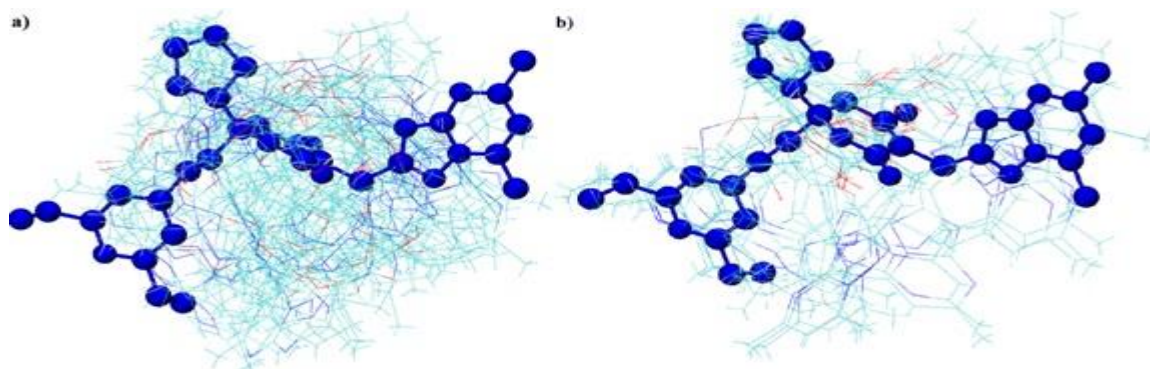


Fig. 3: Alignment of docking conformations generated from a) AutoDock4.2 and a) AutoDock Vina.

*AutoDock Vina docking protocol:* All these ligands were also docked to the enzyme with the help of AutoDock Vina using the same docking parameters except that there is an additional parameter, exhaustiveness which is the time spent by a ligand on the search which may reduce the probability of not finding the global minimum of the scoring function. Another parameter is the energy range that specifies the maximum number of binding modes obtained from the docking calculation and it was set to 1 kcal/mol. The interaction analysis is carried out using the visual molecular dynamics (VMD) program[26].

### Results and Discussion

Fig. 3 illustrates the clusters of all the docking conformations of filibuvir into the thumb region of the enzyme obtained from the AutoDock and AutoDock Vina. In the case of AutoDock, docking poses were generated in the thumb region as directed during the grid setting but none of them was well superposed with the

co-crystallized ligand, which could be attributed to the high degrees of freedom of the ligand (Fig 3a). In the case of AutoDock Vina, the docking conformations were seen as more aligned to the co-crystallized ligand as shown in Fig 3b. Out of 17 conformations, three conformations match well with the native conformation yielding RMSD of more than 1 Å, thus demonstrating the reliability of the docking poses obtained from AutoDock Vina (Fig. 4). Based on the above observation, the docking conformations of another thumb inhibitor “lomibuvir” obtained from AutoDock Vina were analyzed and the best docking pose was supposed to be chosen based on the highest binding free energy. However, it is quite worthy to evaluate the binding pose of lomibuvir in the active site, therefore, its docking conformations were also examined by superposing with the crystal structure of filibuvir, and the docking conformation of lomibuvir was chosen based on the best-superposed structure besides evaluating the binding free energy. In this case, the best binding pose was found to have the highest binding affinity of -6.6 kcal/mol which also overlaid with the co-

crystallized ligand (PDB ID: 3FRZ). However, it is also significant to mention that all the conformations of lomibuvir were docked in the thumb regions and have very close binding affinity in the range between -5.7 to -6.6 kcal/mol. Afterward, the binding pattern of lomibuvir in the active site was evaluated which sheds light on different amino acid residues involved in the stabilization of the inhibitor in the protein's thumb region.

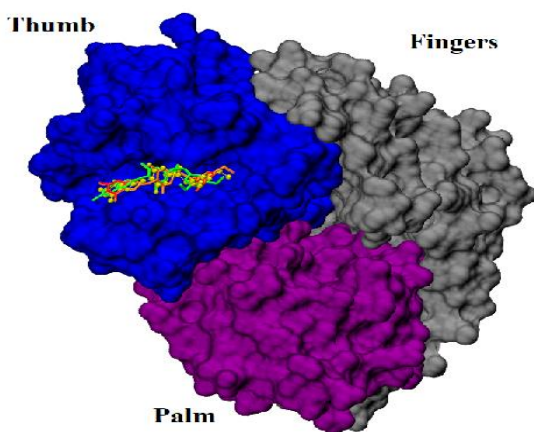
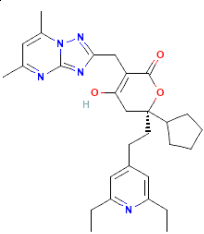
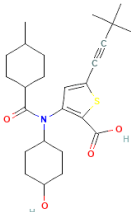


Fig. 4: Superposition of docking conformations of filibuvir with the co-crystallized ligand (yellow) into the thumb region.

Table-1 lists amino acid residues that form different types of interactions with lomibuvir to form a stable protein-ligand complex. The interactions involve

hydrogen bonding as well as hydrophobic contacts which stabilize the ligand into the thumb region of the protein. Ser476, Tyr477, Arg501, and Trp528 are found to interact with the ligand moieties via hydrogen bonding which is shown in Fig. 5. Besides, the ligand is further stabilized with the help of hydrophobic interactions formed between the ligand and non-polar moieties of Met423, Try477, Val485, Ala486, Leu489, Leu497, and Trp528. The strength of the hydrogen bond interactions is evaluated in terms of H-bond lengths and angles which are in the range between 2.50 and 3.50 Å, whereas, for the hydrophobic interactions, the distances have been observed to be greater than 3.50 Å. Analyzing the interaction pattern analysis of lomibuvir in comparison to that of the co-crystallized filibuvir (PDB ID: 3FRZ), the number of amino acid residues involved in providing stability to lomibuvir is found to be less than those in the complex formed between NS5B and filibuvir, since the latter inhibitor has a strong binding affinity in the range between -7.8 to -8.4 kcal/mol for the docking conformations produced in thumb region. Moreover, the number of amino acids involved in providing stability to filibuvir in the protein's thumb region correlated with the X-ray structure examination. Based on the interaction pattern analysis between NS5B and filibuvir, water bridges involving Tyr477, Trp428, and Lys533 as well as π stacking involving His475 are also found to play a significant role in the stabilization of the inhibitor in addition to H-bond interaction and hydrophobic contacts compared to lomibuvir case that has only these two interactions its stability.

Table-1: Binding affinity of thumb inhibitors to NS5B protein and its amino acid residues involved in H-bonding and hydrophobic interactions.

S.no.	Inhibitors	Binding affinity (kcal/mol)	Residues involved in H-bond interaction	Residues involved in hydrophobic contacts
1.	 <p>Filibuvir</p>	-7.8	Ser476 and Arg501	Met423, Try477, Val485, Ala486, Leu489, Leu497 and Trp528
2.	 <p>Lomibuvir</p>	-6.6	Ser476, Tyr477, Arg501 and Trp528	Leu419, Arg422, Met423, Try477, Ile482, Val485, Leu497 and Trp528



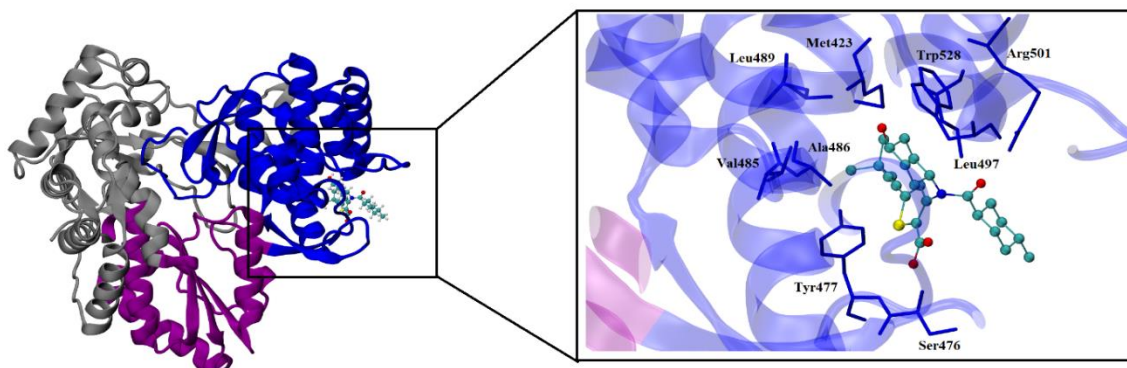


Fig. 5: Interaction pattern of lomibuvir in the thumb region of NS5B protein.

Similarly, the binding pattern of the palm inhibitors is evaluated with the help of molecular docking. However, before binding pattern analysis, the re-docking of the co-crystallized substituted benzothiadiazine to the protein has been analyzed in the case of both molecular docking procedures. In the case of AutoDock, the docking conformations are similarly found to be very deviating as no conformation has been superposed well with the co-crystallized ligand (PDB ID: 3HHK). However, the docking conformations obtained from the AutoDock Vina were found to be matching well with the co-crystallized ligand within the 1 Å limit as shown in Fig. 6, thus validating the docking program for further docking calculations. Therefore, the AutoDock Vina results obtained for the palm inhibitors such as dasabuvir and nesbuvir have been analyzed and interpreted for the possible interaction between the inhibitors and the enzyme.

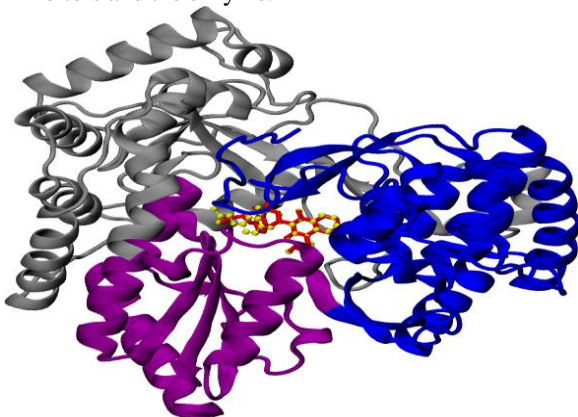


Fig. 6: Superposition of the docking conformation of benzothiadiazine derivative with co-crystallized ligand in the palm region.

Fig. 7 illustrates the binding pattern of dasabuvir in the enzyme's palm region showing different interactions including hydrogen bonding and hydrophobic contacts which are responsible for the ligand's stability during the complex formation. Dasabuvir binding to the enzyme's active site yields a binding affinity of -8.5 kcal/mol. Table-2 shows amino acid residues involved in the interactions with dasabuvir which include H-bond interactions with Asn316 and Asp318, and hydrophobic contacts with Phe193, Asp319, Leu384, Met414, Tyr415, and Tyr448. Another palm inhibitor "nesbuvir" was comparatively assessed to form a weak complex with NS4B protein as deduced from the binding affinity value (-7.1 kcal/mol). A comparative analysis of the stability of the two complexes "nesbuvir-NS5B and dasabuvir-NS5B" reveals a different number of amino acid residues which helps deduce their relative stability. In the case of the nesbuvir-NS5B complex shown in Fig. 8, Asp318 and Tyr448 were involved in H-bonding whereas the inhibitor formed hydrophobic contacts with Leu384, Met414, Tyr415, and Tyr448. Detailed analysis of the interaction profile of these two complexes, the number of H-bond interactions was the same in both cases, whereas contrast is observed in the number of hydrophobic contacts being more in the case of dasabuvir-NS5B complex than nesbuvir-NS5B complex. The stability of these complexes obtained from the docking calculations should also be envisaged in a dynamic environment by utilizing advanced methods like molecular dynamics simulation which could help to gain deeper insight into the dynamic flexibility of the protein due to ligand binding to the protein.

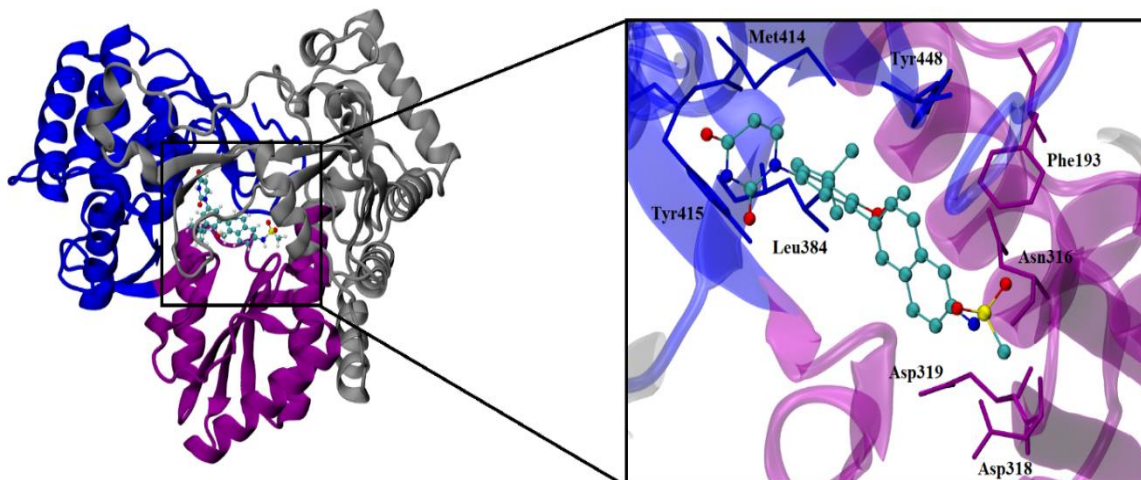


Fig. 7: Interaction pattern of dasabuvir in the palm region of NS5B protein.

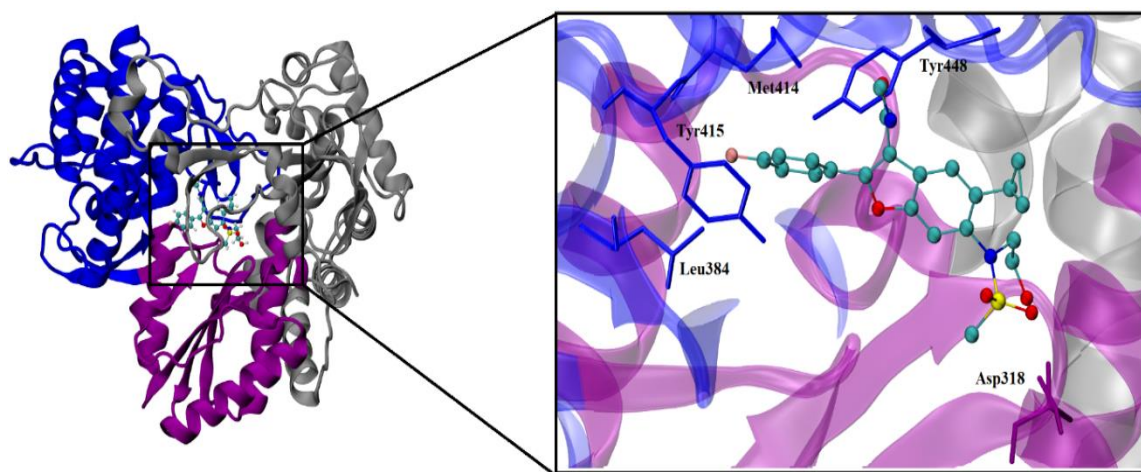
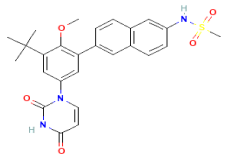
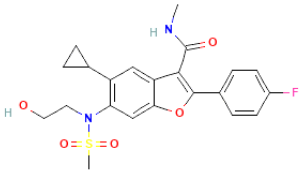


Fig. 8: Interaction pattern of nesbuvir in the palm region of NS5B protein.

Table-2: Binding affinity of palm inhibitors to NS5B protein and its amino acid residues involved in H-bonding and hydrophobic interactions

S.no.	Inhibitors	Binding affinity (kcal/mol)	Residues involved in H-bond interaction	Residues involved in hydrophobic contacts
1.	 Dasabuvir	-8.5	Asn316 and Asp318	Phe193, Asp319, Leu384, Met414, Tyr415 and Tyr448
2.	 Nesbuvir	-7.1	Asp318 and Tyr448	Leu384, Met414, Tyr415 and Tyr448

## Conclusion

Based on the docking calculations, the relative binding strength of non-nucleoside thumb and palm inhibitors was evaluated against the NS5B protein in terms of binding affinity and interaction pattern. The thumb inhibitors “filibuvir and lomibuvir” demonstrate distinct binding patterns which are evident from the nature of the interaction formed between the inhibitors and the proteins. In the case of the filibuvir-NS5B complex, salt bridges and  $\pi$ - $\pi$  stacking interactions were additional stabilizing forces for the inhibitor besides hydrogen bonding and hydrophobic contacts which are the only interactions that are providing stability to lomibuvir. As far as palm inhibitors are concerned, dasabuvir strongly binds to the palm site compared to nesbuvir since the former has a large binding affinity as well as the number of residues involved in the formation of complex formation is more in the case of dasabuvir. The relative stability of all complexes cannot be evaluated since the binding affinity of these complexes is close and would be difficult to estimate based on interaction patterns obtained from the rigid docking. This can be achieved by considering the flexible protein and solvent environment during the implementation of computational methods that can be only circumvented by the application of computer simulations like molecular dynamics simulations. Nevertheless, the results obtained from the docking calculation are very helpful to develop a rationale for how these inhibitors bind to NS5B protein thus leading to its inhibition. Moreover, the current study also implies the possibility of considering its results for the future inhibitor design NS5B genotypes other than 1b.

## References

1. D. Lavanchy, The Global Burden of Hepatitis C, *Liver Int.*, **29**, 74 (2009).
2. J. Dubuisson and F-L. Cosset, Virology and Cell Biology of the Hepatitis C Virus Life Cycle—An Update, *J. Hepatol.*, **61**, S3 (2014).
3. M. Kaito, S. Ishida, H. Tanaka, S. Horiike, N. Fujita, Y. Adachi and M. Kohara, *et al.* Morphology of Hepatitis C and Hepatitis B Virus Particles as Detected by Immunogold Electron Microscopy, *Med. Mol. Morphol.*, **39**, 63 (2006).
4. A. Op De Beeck and J. Dubuisson, Topology of Hepatitis C Virus Envelope Glycoproteins, *Rev. Med. Virol.*, **13**, 233 (2003).
5. R. Jubin, Hepatitis C IRES: Translating Translation into a Therapeutic Target, *Curr. Opin. Mol. Ther.*, **3**, 278 (2001).
6. R. De Francesco, Molecular Virology of the Hepatitis C Virus, *J. Hepatol.*, **31**, 47 (1999).
7. Z. Jin, V. Leveque, H. Ma, K. A. Johnson and K. Klumpp, Assembly, Purification, and Pre-Steady-State Kinetic Analysis of Active RNA-Dependent RNA Polymerase Elongation Complex, *J. Biol. Chem.*, **287**, 10674 (2012).
8. D. Moradpour, F. Penin and C. M. Rice, Replication of Hepatitis C Virus, *Nat. Rev. Microbiol.*, **5**, 453 (2007).
9. K. Rigat, Y. Wang, T. W. Hudyma, M. Ding, X. Zheng, R. G. Gentes and B. R. Beno, *et al.*, Ligand-Induced Changes in Hepatitis C Virus NS5B Polymerase Structure, *Antiviral Res.*, **88**, 197 (2010).
10. J. Dillon, What is the Best Treatment?, *J. Viral Hepat.*, **11**, 23 (2004).
11. H. Ago, T. Adachi, A. Yoshida, M. Yamamoto, N. Habuka, K. Yatsunami and M. Miyano, Crystal Structure of the RNA-Dependent RNA Polymerase of Hepatitis C Virus, *Structure*, **7**, 1417 (1999).
12. S. Bressanelli, L. Tomei, F. A. Rey and R. De Francesco, Structural Analysis of the Hepatitis C Virus RNA Polymerase in Complex with Ribonucleotides, *J. Virol.*, **76**, 3482 (2002).
13. C. A. Lesburg, M. B. Cable, E. Ferrari, Z. Hong, A. F. Mannarino and P. C. Weber, Crystal Structure of the RNA-Dependent RNA Polymerase from Hepatitis C Virus Reveals a Fully Encircled Active Site, *Nat. Struct. Biol.*, **6**, 937 (1999).
14. M. J. Sofia, W. Chang, P. A. Furman, R. T. Mosley and B. S. Ross, Nucleoside, Nucleotide, and Non-Nucleoside Inhibitors of Hepatitis C Virus NS5B RNA-Dependent RNA-Polymerase, *J. Med. Chem.*, **55**, 2481 (2012).
15. M. L. Barreca, N. Iraci, G. Manfroni and V. Cecchetti, Allosteric Inhibition of the Hepatitis C Virus NS5B Polymerase: In Silico Strategies for Drug Discovery and Development, *Future Med. Chem.*, **3**, 1027 (2011)
16. H. Khalid, S. Shahid, S. Tariq, B. Ijaz, U. A. Ashfaq and M. Ahmad, Discovery of Novel HCV NS5B Polymerase Inhibitor, 2-(3, 4-Dimethyl-5, 5-Dioxidobenzo [e] Pyrazolo [4, 3-c][1, 2] Thiazin-2 (4 H)-yl)-N-(2-Fluorobenzyl) Acetamide via Molecular Docking and Experimental Approach, *Clin. Exp. Pharmacol.*, **48**, 1653 (2021).
17. Z. Wang, Z. Chen, J. Li, J. Huang, C. Zheng and J-P. Liu, Combined 3D-QSAR, Molecular Docking and Molecular Dynamics Study on the Benzimidazole Inhibitors Targeting HCV NS5B Polymerase, *J. Biomol. Struct. Dyn.*, **38**, 1071 (2020).
18. M. Zhong, E. Peng, N. Huang, Q. Huang, A. Huq, M. Lau and R. Colonna, *et al.*, Discovery of Novel Potent HCV NS5B Polymerase Non-Nucleoside



- Inhibitors Bearing a Fused Benzofuran Scaffold, *Bioorganic Med. Chem. Lett.*, **28**, 963 (2018).
19. E. Abdurakhmanov, S. Øie Solbak and U. H. Danielson, Biophysical Mode-of-Action and Selectivity Analysis of Allosteric Inhibitors of Hepatitis C Virus (HCV) Polymerase, *Viruses*, **9**, 151 (2017).
  20. J. J. P. Stewart, Optimization of Parameters for Semiempirical Methods I. Method, *J. Comput. Chem.*, **10**, 209 (1989).
  21. J. J. P. Stewart, Optimization of Parameters for Semiempirical Methods II. Applications, *J. Comput. Chem.*, **10**, 221 (1989).
  22. H. Li, J. Tatlock, A. Linton, J. Gonzalez, T. Jewell, L. Patel and S. Ludlum, *et al.*, Discovery of (R)-6-Cyclopentyl-6-(2-(2, 6-Diethylpyridin-4-yl) Ethyl)-3-((5, 7-Dimethyl-[1, 2, 4] Triazolo [1, 5-a] Pyrimidin-2-yl) Methyl)-4-Hydroxy-5, 6-Dihydropryan-2-One (PF-00868554) As a Potent and Orally Available Hepatitis C Virus Polymerase Inhibitor, *J. Med. Chem.*, **52**, 1255 (2009).
  23. A. N. Shaw, R. Tedesco, R. Bambal, D. Chai, N. O. Concha, M. G. Darcy, D. Dhanak, *et al.*, Substituted Benzothiadiazine Inhibitors of Hepatitis C Virus Polymerase, *Bioorganic Med. Chem. Lett.*, **19**, 4350 (2009).
  24. S. Forli, R. Huey, M. E. Pique, M. F. Sanner, D. S. Goodsell and A. J. Olson, Computational Protein–Ligand Docking and Virtual Drug Screening With the AutoDock Suite, *Nat. Protoc.*, **11**, 905 (2016).
  25. O. Trott and A. J. Olson, AutoDock Vina: Improving the Speed and Accuracy of Docking With a New Scoring Function, Efficient Optimization, and Multithreading, *J. Comput. Chem.*, **31**, 455 (2010).
  - W. Humphrey, A. Dalke and K. Schulten, VMD - Visual Molecular Dynamics, *J. Molec. Graphics*, **14**, 33 (1996).